Ridge Detection and Perceptual Grouping Based Automatic Counting of Rice Seedlings Using UAV Images

Jianyuan Ni[1], Zanbo Zhu[1], Xin-Gen Zhou[2], Fugen Dou[2], Yubin Yang[2], Lloyd T. Wilson[2], Stanley Omar PB. Samonte[2], Jing Wang[2], Jing Zhang[1]
[1]*Computer Science Department, Lamar University, Beaumont, TX 77710, USA*
[2]*Texas A &M AgriLife Research Center, Beaumont, TX 77713, USA*
jni@lamar.edu, zzhu4@lamar.edu, Shane.Zhou@aesrg.tamu.edu, Fugen.Dou@aesrg.tamu.edu, yubin.yang@aesrg.tamu.edu, LT.Wilson@aesrg.tamu.edu, Stanley.Samonte@ag.tamu.edu, jingw@aesrg.tamu.edu, jzhang9@lamar.edu

2021 6th International Conference on Image, Vision and Computing (ICIVC) | 978-1-6654-4368-5/21/$31.00 ©2021 IEEE | DOI: 10.1109/ICIVC52351.2021.9526939

***Abstract*—Automatic counting of rice seedling stand is desirable but challenging. In this paper, we propose a new method to detect and count drill-seeded, delay-flooded rice seedlings using unmanned aerial vehicle (UAV) images. First, a coarse-to-fine dual scale ridge detection method is developed to detect individual rice research plot at a coarse scale and its associated rice seedlings at a fine scale. Then, the skeleton of each detected rice seedling region is extracted and separated into small skeleton segments for rice seedling structure analysis. Finally, the skeleton segments are grouped based on seedling structure by a graph-cut based perceptual grouping. We evaluated the proposed method using more than 20,000 rice seedlings from 20 UAV images and the results demonstrated that our method can detect and count rice seedling with a high average accuracy of 89.37%.**

Keywords—rice seedlings counting, unmanned aerial vehicle, ridge detection, perceptual grouping

I. Introduction

Rice is an important primary staple food in the world and its consumption accounts for more than half of the daily caloric intake of over three billion people. Agricultural research that helps to ensure the security and continued increase in rice production is crucial to meeting the growing global demand for rice.

Rice seedling density is a critical agronomic component for rice production it greatly impacts yield potential and it determines the crop's response to insect, disease, and weed pests. Traditionally seedling density is estimated based on manual counting of rice seedlings, which is not only extremely tedious and time-consuming, but also greatly constrained by personnel, subjectivity, and weather conditions. Therefore, there is a need to develop a fast, low-cost, and reliable method that can accurately estimate rice seedling density.

Digital agricultural research has been receiving an increasing attention due to the rapid development in innovative computer techniques, such as computer vision, machine learning, and artificial intelligence. Several image-based plant counting methods that have been reported. Fernandez-Gallego et al. [1] developed a method to count wheat ears using a Laplacian frequency enhancement and a median filter to remove the soil and leaves. Zhou et al. [2] proposed another wheat ear counting method that separated the image into wheat ear and background by a cluster method, and then classified each pixel based on color and texture using a trained twin-support-vector machine. In the method presented by Guo et al. [3], a two-step voting based machine learning method used color and features from a gray level co-occurrence matrix to train a pixel level segmentation model, which segmented the image into sorghum and non-sorghum head regions for counting. Tao et al. [4] used Otsu's thresholding method and a chain code-based skeleton optimization method to count wheat seedlings in images.

Unmanned aerial vehicle (UAV), as a new remote sensing tool, has begun to be used more frequently in various agricultural studies, such as crop disease detection and monitoring, pest surveillance, biomass estimation, fertilizer spraying, and water status analysis [5]-[9]. UAV can capture large-scale crop fields efficiently with accurate GPS information and dramatically save human power, time, and cost. For rice seedling counting, Reza et al. applied a median filter and a morphological operation to count rice seedlings by detecting connected components in UAV images [10]. Wu et al. used a basic and a combined deep learning network models for rice seedling counting using images captured by a UAV [11]. However, both studies focused on transplanted rice seedlings, which have much larger seedling spacing and lower seedling density compared to drill-seeded rice seedlings in the current study.

(a) (b) (c)

Fig. 1. Challenges for counting drill-seeded rice seedlings. (a) Blurred seedling, (b) Clustered seedlings, and (c) Water reflection.

In this paper, we present a new method to automatically count drill-seeded rice seedlings from UAV images. Automatic counting of drill-seeded seedlings present several major challenges: (1) UAV images typically have lower resolution and therefore are not as clear as still images taken on the ground (Fig. 1-a); (2) drill-seeded rice seedlings usually have high densities and many seedlings are often clustered together (Fig. 1-b); and (3) rice fields have complex background, such as cracks caused by dry soil and water reflection (Fig. 1-c).

Our contributions are summarized as follows: (1) this is the first study to count drill-seeded rice seedling from UAV images; (2) we have developed a new coarse-to-fine dual-scale ridge detection method for rice field plot and rice seedling detection; and (3) we use a graph cut-based perceptual grouping for high-accuracy individual rice seedling counting.

II. Methodology

The proposed drilled rice seedling counting method consists of three major steps as shown in Fig. 2. The details of each step will be described in the rest of this section.

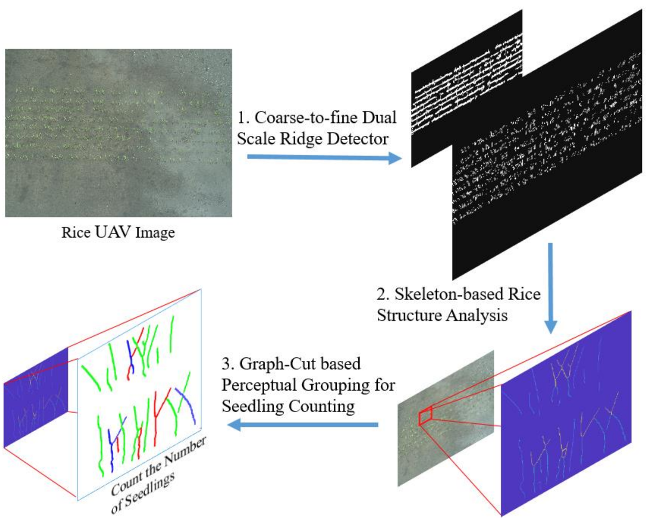

Fig. 2. The flowchart of the rice seedling counting method.

A. Rice Detection Using Dual-Scale Ridge Detector

Ridge points are the points that have local maximum or minimum of principal curvature of a smooth function. The ridge points of an image can be detected by calculating the eigenvalues of a Hessian matrix composed of the second order directional derivatives of the convolution of the image and a Gaussian function [12]. The detected ridge points can be linked to form a curve, which captures both local and global structural information of elongated objects in the image by adjusting the scale level of the Gaussian function.

In this study, we propose a coarse-to-fine dual-scale ridge detection method to extract rice field regions and then rice seedling regions from UAV images based on the facts that: (1) rice seedlings were planted in rows with a large fixed row spacing, and small variable seedling spacing. The seedlings in each row become connected after a broad Gaussian filtering and form an elongated object. Therefore, rice fields can be detected by a coarse-scale ridge detection; and (2) rice seedlings have a long narrow shape that can be considered as elongated objects at a fine scale. Therefore, they can be detected by a fine-scale ridge detection. Algorithm 1 lists the steps of our rice seedling detection.

Algorithm 1: Ridge-based Rice Seedling Detection

(1) Convert the input UAV image from RGB to L*a*b space and the a* channel is used for detection.
(2) Apply a coarse-scale ridge detection and a morphological close operation with a horizontal structure element to extract rice rows.
(3) Use a Hysteresis-based double thresholding method to segment rice rows from the image.
(4) Apply a fine-scale ridge detection to detect rice seedling regions based on the rice seedling rows detected in Step (4).
(5) Use a Hysteresis-based double thresholding method to segment rice seedlings from the image.

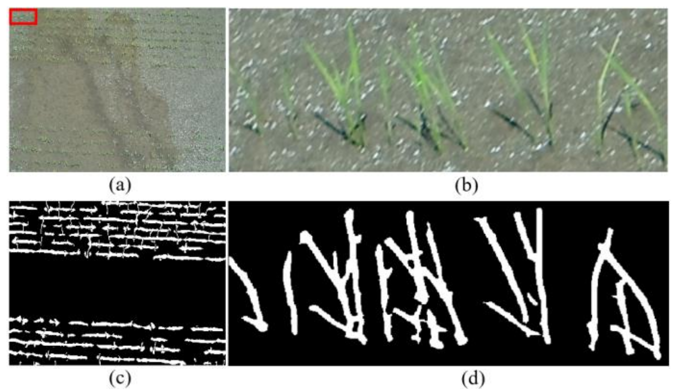

Fig. 3. Ridge-based rice seedling detection.

Fig. 3-(a) shows a UAV image and Fig. 3-(b) is a close-up of the region bounded in the red box in Fig. 3-(a). Fig. 3-(c) and (d) are the rice row and rice seedlings detected by Algorithm 1. The results show that our method can extract rice seedlings accurately, including the first two very blurred ones. However, seedling shadows are also detected and need to be removed before counting.

B. Rice Seedling Structure Analysis Using Skeletons

Each rice seedling region detected in Section 2.1 can be considered as a connected component. However, these connected components cannot be used for rice seedling counting directly because one component may be composed of several connected seedlings. For example, the last connected component in Fig. 3-(d) has three rice seedlings.

We divide the skeleton of each connected component into small meaningful segments for seedling structure analysis based on the following steps:

(1) A medial axis transform is applied to each connected component to extract its skeleton, which can simplify each component while keeping its essential structure.

(2) Two types of key point are extracted for every skeleton obtained in Step (1):

- Skeleton End Point: a skeleton point that has only one skeleton point in its 8-connected neighborhood.
- Skeleton Branch Point: a skeleton point that is the intersection of two or more skeletons.

For rice seedlings, a skeleton end point corresponds the bottom of a seedling or the end point of a leaf, and a skeleton branch point corresponds to the intersection of two leaves or stems.

(3) Skeletons are divided into small segments using the key points detected in Step (2). The length and the mean RGB color of each skeleton segment are calculated to remove too small and non-seedling skeleton segments by a green color thresholding, which results in the removal of shadow skeletons in black.

(4) Skeleton segments are categorized into four classes based on the types of their upper and lower end points, as listed in Table I.

TABLE I. FOUR CLASSES OF SKELETON SEGMENTS

Segment's upper end point	Segment's lower end point	Segment Class
Skeleton End Point	Skeleton End Point	*EE*
Skeleton End Point	Skeleton Branch Point	*EB*
Skeleton Branch Point	Skeleton End Point	*BE*
Skeleton Branch Point	Skeleton Branch Point	*BB*

Fig. 4-(a) shows rice seedlings with their skeletons in red color. Fig. 4-(b) illustrates the skeleton segments after the removal of shadow skeletons. The detected skeleton end points and skeleton branch points are marked as green and red crosses. The 1st skeleton has 1 EE segment, the 2nd skeleton has 1 EE and 2 EB segments, and the last skeleton has 3 BE, 1 BB, and 1 EB segments.

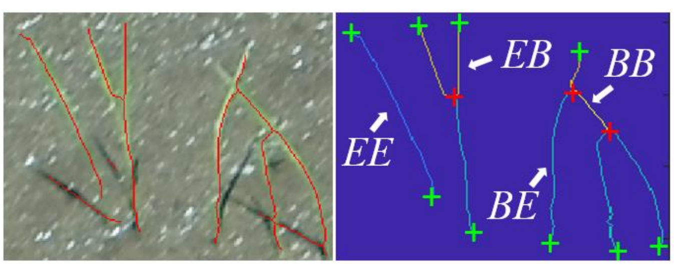

(a) (b)

Fig. 4. Seedling Skeletons and their segments.

By analyzing the skeleton segments of rice seedling, we can see that different segments represent different parts of a rice seedling. EE and BE segments typically represent seedling stems, EB segments typically represent seedling leaves, and BB segments typically represent the connection part between stem and leaf. Therefore, each individual rice seeding can be extracted by grouping the parts from the same rice seedling together.

C. Seedling Counting Using Perceptual Grouping

Inspired by the edge grouping method presented in [13], we modified a graph based perceptual grouping method to group rice seeding skeleton segments.

Each skeleton can be converted to a weighted graph *G(V,E)*. Every segment of a skeleton is a vertex in the vertex set *V* and there is a link in the edge set *E* between every two connected segments.

Two Gestalt principles, proximity and continuity, are calculated as follows to indicate the likelihood of grouping the segments together:

(1) Proximity, which measures the distance between two segments. Because any two segments in a skeleton are connected directly or via one or more other segments, the distance between two segments is the number of skeleton points connecting them. If two segments share an end point, the distance between them is zero.

(2) Continuity, which measures the orientation difference of two segments. The segment orientation is the angle between the x-axis and the major axis of the ellipse that has the same second moments as the segment.

The weight of a link is computed using a RankSVM trained by a large scale human-drawn sketch dataset [14]. The RankSVM can give a larger link score to a link if the two vertices of that link are more likely to be grouped together based on their proximities and continuities.

After constructing the graph using skeleton segments, the rice seedling segmentation is treated as a graph partition problem, which can be solved as a min-cut optimization problem by minimizing an overall energy below [13]:

$$E(v_L) = \sum_{v_i \in V} D(v_i, v_L) + \sum_{\{v_i, v_j\} \in N} S(v_i, v_j)$$

where,

$$D(v_i, v_L) = sigmoid(Link\ sore\ between\ v_i\ and\ v_L)^{-1}$$

$$S(v_i, v_j) = d(v_i, v_j)^{-1}$$

V_L is a set of cluster centers that correspond to EE and BE segments in the graph because they have high probabilities to be rice seedling stems. $D(V_I, V_L)$ is the energy measuring how close the two vertices in the Gestalt space, which is indicated by an inverse sigmoid function on the link score produced by the RankSVM. N is the set of neighboring vertices of V_I in V. $S(V_I, V_J)$ is the energy measuring the spatial correlation between two neighboring vertices, which is computed as the inverse Euclidean hausdorff-distance function between them. Two inverse functions are used here to fit the minimization problem defined by the min-cut problem for graph partition.

Fig. 5 shows an example with 8 detected rice seedling regions that have 1, 1, 7, 1, 9, 1, 3, and 5 skeleton segments, respectively. After grouping, a total of 12 rice seedling are detected.

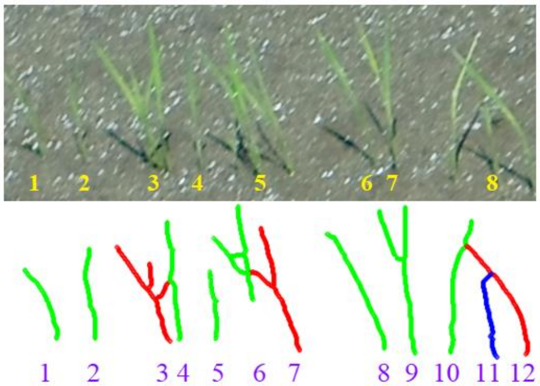

Fig. 5. Graph-cut-based perceptual grouping results.

III. EXPERIMENTS

A. UAV Image Dataset

Twenty UAV images with more than 20,000 rice seedlings were collected at the Texas A&M AgriLife Research Center in Beaumont, TX, USA using a Zenmuse X7 24 MP camera mounted on a DJI Inspire 2 flying at an altitude of 7 m and a 60˚ angle between the camera and ground. All images have a 3936×5248 pixel resolution.

The ground truth data (i.e., the number of rice seedlings) of the selected UAV images were manually counted by an experienced rice research technician at the Texas A&M AgriLife Research Center. The number of rice seedlings in the 20 images ranges from 532 to 1391.

B. Evaluation Metrics and Experimental Settings

The absolute error (AE) and accuracy (Acc) defined below were used as evaluation metrics to assess the performance of the proposed method.

$$\mathrm{AE} = |t_i - c_i|$$

$$\mathrm{Accuracy} = \left(1 - \frac{|t_i - c_i|}{t_i}\right) \times 100\%$$

T_I is the ground truth of the I^{TH} image and C_I is the output of the proposed method $(1 \leqslant I \leqslant 20)$. The lower the AE, the better the counting performance, and the higher the Acc, the better the counting performance.

In our experiments, the coarse and fine scales of Gaussian function were 50 and 2.5. The Hysteresis-based thresholding values were 0.15 and 0.24 for rice row detection and 0.14 and 0.23 for seedlings. The skeleton segments with length smaller than 30 pixels were removed. All parameters were determined experimentally.

C. Experimental Results

The experimental results of 20 images with more than 20,000 rice seedlings are listed in Table II. Fig. 6 illustrates the number of rice seedlings of each image given by the ground truth and our method.

TABLE II. ABSOLUTE ERROR AND ACCURACY OF 20 IMAGES

Image ID	AE	Acc	Image ID	AE	Acc
1	11	99.11%	11	27	97.74%
2	16	98.26%	12	154	82.96%
3	57	95.79%	13	70	92.16%
4	69	93.72%	14	33	93.80%
5	66	93.86%	15	244	75.28%
6	33	97.62%	16	161	80.27%
7	135	87.05%	17	180	82.56%
8	40	96.31%	18	207	77.86%
9	102	90.87%	19	196	80.82%
10	100	88.57%	20	145	82.84%

Since this is the first study to count drill-seeded rice seedling from UAV images, no other methods can be used for performance comparison. We believe our method achieved good performance on this very challenging task. The average accuracy of 20 images is 89.37%, which reflects the current state-of-the-art. Moreover, it can serve as a baseline method for future research in this area. We also noticed that the performance of the first 14 images (average accuracy 93.42%) is better than that of the last six images (average accuracy 79.94%). Many seedlings were not detected in the last six images. The reason is that the last six images have large part of the background region covered by water with strong reflection, which increased the difficulty to detect the rice seedlings. Fig. 7 shows two parts from the 1st and 15th images, demonstrating the increased difficulty detecting seedlings from the 15th image.

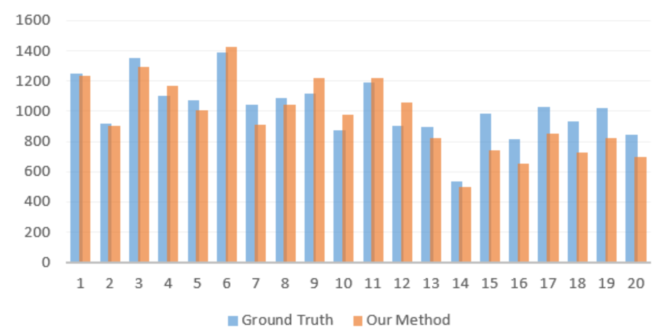

Fig. 6. Ground truth versus the method output of 20 images.

Fig. 7. Two parts from the 1st image and the 15th image.

IV. CONCLUIONS AND FUTURE WORK

Maintaining a sufficient rice seedling stand is critical to approach the yield potential of a cultivar in drill-seeded, delay-flooded production. Traditional seedling density estimation is based on manual seedling counting, which is very time-consuming and its counting accuracy affected by many factors. In this paper, we presented the first automatic method in the literature to count drill-seeded rice seedlings using UAV images. An efficient coarse-to-fine dual-scale detection method is developed to detect rice fields and rice seedling regions based on their shape properties. To extract each rice seedling from clusters of seedlings, a graph-cut based perceptual grouping method is applied to group the skeleton segments from the same seedling together based on a seedling structure analysis. The proposed method was evaluated using 20 rice UAV images and achieved high (approximately 90%) counting accuracy.

In our future work, we will continue to improve the rice seedling detection method to make it robust to water background reflection, soil cracking, solar reflectance, and seedling stage. We will also include more structure features to strengthen perceptual grouping to further increase the rice seedling counting accuracy.

ACKNOWLEDGEMENT

We gratefully acknowledge the high performance computing cluster supported by the U.S. National Science Foundation (Award No. 1726500) used for this research. Any opinions, findings, and conclusions or recommendations expressed in this material are those of the authors and do not necessarily reflect the views of the funding agency.

REFERENCES

[1] Fernandez-Gallego, Jose A., Shawn C. Kefauver, Nieves Aparicio Gutiérrez, María Teresa Nieto-Taladriz, and José Luis Araus. "Wheat ear counting in-field conditions: high throughput and low-cost approach using RGB images." *Plant methods* 14, no. 1 (2018): 22.

[2] Zhou, Chengquan, Dong Liang, Xiaodong Yang, Hao Yang, Jibo Yue, and Guijun Yang. "Wheat ears counting in field conditions based on multi-feature optimization and TWSVM." *Frontiers in plant science* 9 (2018): 1024.

[3] Guo, Wei, Bangyou Zheng, Andries B. Potgieter, Julien Diot, Kakeru Watanabe, Koji Noshita, David Jordan et al. "Aerial Imagery Analysis—Quantifying Appearance and Number of Sorghum Heads for Applications in Breeding and Agronomy." *Frontiers in plant science* 9 (2018): 1544.

[4] Liu, Tao, Wei Wu, Wen Chen, Chengming Sun, Xinkai Zhu, and Wenshan Guo. "Automated image-processing for counting seedlings in a wheat field." *Precision agriculture* 17, no. 4 (2016): 392-406.

[5] Calderón, Rocío, Juan Navas-Cortés, and Pablo Zarco-Tejada. "Early detection and quantification of Verticillium wilt in olive using hyperspectral and thermal imagery over large areas." Remote Sensing 7, no. 5 (2015): 5584-5610.

[6] Jannoura, Ramia, Katja Brinkmann, Daniel Uteau, Christian Bruns, and Rainer Georg Joergensen. "Monitoring of crop biomass using true colour aerial photographs taken from a remote controlled hexacopter." Biosystems Engineering 129 (2015): 341-351.

[7] Vanegas, Fernando, Dmitry Bratanov, Kevin Powell, John Weiss, and Felipe Gonzalez. "A novel methodology for improving plant pest surveillance in vineyards and crops using UAV-based hyperspectral and spatial data." Sensors 18, no. 1 (2018): 260.

[8] Schut, Antonius GT, Pierre C. Sibiry Traore, Xavier Blaes, and A. Rolf. "Assessing yield and fertilizer response in heterogeneous smallholder fields with UAVs and satellites." Field Crops Research 221 (2018): 98-107.

[9] Santesteban, L. G., S. F. Di Gennaro, A. Herrero-Langreo, C. Miranda, J. B. Royo, and A. Matese. "High-resolution UAV-based thermal imaging to estimate the instantaneous and seasonal variability of plant water status within a vineyard." Agricultural Water Management 183 (2017): 49-59.

[10] Reza, Md Nasim, In Seop Na, and Kyeong-Hwan Lee. "Automatic counting of rice plant numbers after transplanting using low altitude uav images." *International Journal of Contents* 13, no. 3 (2017): 1-8.

[11] Wu, Jintao, Guijun Yang, Xiaodong Yang, Bo Xu, Liang Han, and Yaohui Zhu. "Automatic Counting of in situ Rice Seedlings from UAV Images Based on a Deep Fully Convolutional Neural Network." *Remote Sensing* 11, no. 6 (2019): 691.

[12] Staal, Joes, Michael D. Abràmoff, Meindert Niemeijer, Max A. Viergever, and Bram Van Ginneken. "Ridge-based vessel segmentation in color images of the retina." *IEEE transactions on medical imaging* 23, no. 4 (2004): 501-509.

[13] Qi, Yonggang, Yi-Zhe Song, Tao Xiang, Honggang Zhang, Timothy Hospedales, Yi Li, and Jun Guo. "Making better use of edges via perceptual grouping." In *Proceedings of the IEEE conference on computer vision and pattern recognition*, pp. 1856-1865. 2015.

[14] Eitz, Mathias, James Hays, and Marc Alexa. "How do humans sketch objects?." *ACM Transactions on graphics (TOG)* 31, no. 4 (2012): 1-10.